

# A SIMPLIFIED ORTHO-RECTIFICATION APPROACH FOR SATELLITE IMAGERY

X. Wu

CSIRO Mathematical and Information Sciences, 65 Brockway Road, Floreat, WA, 6014, Australia  
Phone +61 8 9333 6162, Fax +61 8 9333 6121, Xiaoliang.Wu@csiro.au

## Commission III, WG III/1

**KEY WORDS:** Satellite, Sensor, Pushbroom, Estimation, Landsat, SPOT

### ABSTRACT:

A novel ortho-rectification approach for satellite imagery, which we name the 'three-model approach', is proposed. Rather than fitting a single model, as is typically done, this approach fits a sequence of three models. The first model estimates the azimuth of the image, the image scaling factor and image shifting; the second model estimates the overall image pitch/shearing angle; and the third model estimates the image roll and swing angles and the affine transformation coefficients. The first and second models are linear while the third model is non-linear. Unlike other ortho-rectification approaches which require sensor and orbital ephemeris information and large numbers of control points, the three-model approach requires only the rough satellite orbit height above the earth's surface and a minimum of only four control points for the whole process.

In experimental trials, this new approach has been tested and compared with established implementations of rigorous satellite orbital modelling. Overall, the results from the three-model approach for satellite image ortho-rectification are promising in comparison to the rigorous satellite orbital modelling. The three-model approach is easy to understand (it has a clear physical meaning for each model) and the implementation is very simple. The biggest advantage of the three-model approach over other approaches is that it does not require good approximations for parameters and other associated information (such as ephemeris data). In addition, to ensure minimal residuals within a production environment, the proposed three-model approach employs a robust estimation technique. Results from several trials demonstrated that the proposed approach is a good alternative for real production work.

## 1. INTRODUCTION

Rigorous modelling approaches for satellite imagery can be found in many references (Salamonowicz, 1986; Bannari et al, 1995; Al-Rousan et al, 1997, Toutin, 1992; Toutin et al, 2003), and are now implemented in commercial software. In general, sufficient ground control points and detailed satellite orbital information including ephemeris data hold the key for accurately modelling the relationship between satellite image coordinates and ground coordinates.

Depending on how the variety of orbital parameters are modelled, rigorous ortho-rectification models usually have two or three times the number of unknowns/parameters compared to conventional frame models (usually only six exterior orientation parameters for frame-based image ortho-rectification). Obviously, more unknowns/parameters means that more ground control points are required. Furthermore, because the rigorous ortho-rectification models are usually obtained after differentiating the collinearity equations, good approximations for parameters are often needed. If the provided coordinates of the ground control points are based on a map-projection coordinate system (e.g. easting, northing and height in a UTM zone), then an additional coordinate transformation is required to convert the map-projection coordinates into the object space coordinates. The large number of unknowns and the requirement for good approximations for unknowns can make these rigorous models difficult to implement in practice.

Besides rigorous models, using fitted polynomials, rational functions, or their derivative functions for satellite imagery ortho-rectification are currently quite popular (Grodecki, 2001). However, these methods are purely numerical fits between the ground control points and their image points. Due to many coefficients that are usually involved, such methods require large numbers of ground control points in order to solve for the coefficients. Also the kinds of coefficients to be included in the fitting models are terrain-dependent.

A novel ortho-rectification approach for satellite imagery, which we name the 'three-model approach', is proposed. Rather than fitting a single model, as is typically done, this approach fits a sequence of three models. The first model estimates the azimuth of the image, the image scaling factor and image shifting; the second model estimates the overall image pitch/shearing angle; and the third model estimates the image roll and swing angles and the affine transformation coefficients. The first and second models are linear while the third model is non-linear. Unlike other ortho-rectification approaches which require sensor and orbital ephemeris information and large numbers of control points, the three-model approach requires only the rough satellite orbit height above the earth's surface and a minimum of four control points for the whole process. It does not require: 1) any imaging sensor details such as the focal length or the pixel size; 2) the satellite orbit information such as the approximations of the satellite positions and view angle; and

3) additional coordinate transformations between map-projection coordinate systems and local coordinate systems.

In experimental trials, this approach has been tested and compared with established implementations of rigorous satellite orbital modelling. This paper will present the method, the experimental results and aspects of the operational implementation of the three-model approach for production work. The paper is organized as follows: first the fundamentals of rigorous models are introduced, then the three-model approach is described in detail, then some experimental results are presented and finally some future work is discussed.

## 2. RIGOROUS ORTHO-RECTIFICATION APPROACHES

The rigorous modelling approaches for satellite image ortho-rectification are basically derived from the geometric relationship between the ground control points and their corresponding image points. A rotation matrix  $R$  is used to determine the transformational relationship between the image space coordinates  $(x, y, z = -f)$  ( $f$  is the focal length) and the object space coordinates  $(X, Y, Z)$ . The rotation matrix  $R$  based on the  $A, \gamma, k$  rotation system is chosen because it is commonly used in single-image photogrammetry (Wang, 1990, p.2). The three rotation angles  $A, \gamma, k$  represent the azimuth of the image, the image roll angle and the image swing angle, respectively. The rotation matrix  $R$  is defined as

$$R = \begin{bmatrix} a_1 & a_2 & a_3 \\ b_1 & b_2 & b_3 \\ c_1 & c_2 & c_3 \end{bmatrix} = \begin{bmatrix} \cos A & -\sin A & 0 \\ \sin A & \cos A & 0 \\ 0 & 0 & 1 \end{bmatrix} \begin{bmatrix} \cos \gamma & 0 & -\sin \gamma \\ 0 & 1 & 0 \\ \sin \gamma & 0 & \cos \gamma \end{bmatrix} \begin{bmatrix} \cos k & -\sin k & 0 \\ \sin k & \cos k & 0 \\ 0 & 0 & 1 \end{bmatrix} = \begin{bmatrix} \cos A \cos \gamma \cos k - \sin A \sin k & \cos A \cos \gamma \sin k - \sin A \cos k & -\cos A \sin \gamma \\ \sin A \cos \gamma \cos k + \cos A \sin k & -\sin A \cos \gamma \sin k + \cos A \cos k & -\sin A \sin \gamma \\ \sin \gamma \cos k & -\sin \gamma \sin k & \cos \gamma \end{bmatrix}$$

The transformational relationship from an image point  $(x, y, -f)$  to its object space coordinates  $(X, Y, Z)$  is given by:

$$\begin{bmatrix} X - X_s \\ Y - Y_s \\ Z - Z_s \end{bmatrix} = \lambda \begin{bmatrix} u \\ v \\ w \end{bmatrix} = \lambda R(A, \gamma, k) \begin{bmatrix} x \\ y \\ -f \end{bmatrix} = \lambda \begin{bmatrix} a_1 & a_2 & a_3 \\ b_1 & b_2 & b_3 \\ c_1 & c_2 & c_3 \end{bmatrix} \begin{bmatrix} x \\ y \\ -f \end{bmatrix} \quad (1)$$

where  $(X_s, Y_s, Z_s)$  are the satellite or projection centre coordinates,  $(u, v, w)$  are the auxiliary space coordinates of an image point  $(x, y, -f)$ , and  $\lambda$  is a scaling factor which varies for an individual point. Eliminating  $\lambda$  from (1) and taking into account  $R^T = R^{-1}$ , the so-called collinearity equations in photogrammetry result:

$$\begin{aligned} x &= x_0 - f \frac{a_1(X - X_s) + b_1(Y - Y_s) + c_1(Z - Z_s)}{a_3(X - X_s) + b_3(Y - Y_s) + c_3(Z - Z_s)} \\ y &= y_0 - f \frac{a_2(X - X_s) + b_2(Y - Y_s) + c_2(Z - Z_s)}{a_3(X - X_s) + b_3(Y - Y_s) + c_3(Z - Z_s)} \end{aligned} \quad (2)$$

where  $x_0, y_0$  are the image plane coordinates of the camera principal point and  $a_i, b_i, c_i (i=1,2,3)$  are the nine elements in the rotation matrix. The collinearity equations (2) are considered as the fundamental equations in photogrammetry and are also the core of the ortho-rectification processing.

There is only one projection centre and one rotation matrix for frame-grabbed imagery such as aerial photography and video images. However, since the imagery is formed from scan-lines for most satellite imagery (e.g. Landsat, SPOT, IKONOS, QuickBird, etc.), the projection centre and the rotation matrix varies line by line (strictly even pixel by pixel for mirror scanning modes such as Landsat sensors). In order to estimate the projection centre and the rotation matrix accurately, it is common practice to assume that the projection centre and rotation angles vary proportionally with respect to time or scan-line.

Rigorous modelling approaches can be found in (Salamonowicz, 1986; Bannari et al, 1995; Al-Rousan et al, 1997; Toutin, 1992; Toutin, et al, 2001, 2003). In general, sufficient ground control points and detailed satellite orbital information (including ephemeris data) hold the key for accurately modelling the relationship between satellite image coordinates and ground coordinates.

Depending on how the variety of orbital parameters are modelled, these rigorous ortho-rectification models usually have two or three times the number of unknowns/parameters compared to conventional frame models (Salamonowicz, 1986). Obviously, more unknowns/parameters means that more ground control points are required. Furthermore, because the rigorous ortho-rectification models are usually obtained after differentiating the collinearity equations, good approximations for parameters are often needed. If the provided coordinates of the ground control points are based on a map-projection coordinate system (e.g. easting, northing and height in a UTM zone), then an additional coordinate transformation is required to convert the map-projection coordinates into the object space coordinates  $(X, Y, Z)$ . The large number of unknowns and the requirement for good approximations for unknowns can make these rigorous models difficult to implement in practice.

In this paper, we introduce a novel three-model approach (see Section 3). It does not require satellite orbital information except for a rough satellite orbital height. In addition, the proposed approach has physical meanings for the model parameters.

## 3. THE THREE-MODEL APPROACH

The proposed approach is to separate the ortho-rectification process into the fitting of three consecutive models instead of a single-model fitting process typically used by many satellite ortho-rectification methods. The first model aligns the imagery with the ground coordinate system by rotating and scaling the imagery, the second model adjusts the overall pitch angle, and the third model removes the image distortion caused by the sensor's perspective view angles and the terrain undulation.

The basic assumption of the proposed three-model approach is that the satellite imaging sensor is far from the ground. This is true for most remote sensing satellites where orbital heights are usually around 300 to 900 kilometres above the earth's surface. From this assumption, the first model can be derived.

### 3.1 First Model

From (1), if the third row of the matrices is ignored and the properties of the rotation matrix  $R$  are taken into account, then the following relationship can be derived:

$$\sin A \cdot X - \cos A \cdot Y + \lambda \sin k \cdot x + \lambda \cos k \cdot y - (\sin A \cdot X_s - \cos A \cdot Y_s) = 0$$

$$b_3 X - a_3 Y + \lambda c_2 x - \lambda c_1 y - b_3 X_s + a_3 Y_s = 0 \quad (3)$$

Assuming that the scaling factor  $\lambda$  is constant for all points, then (3) can be rewritten as:

$$k_0 X + k_1 Y + k_2 x + k_3 y + 1 = 0 \quad (4)$$

where  $k_0, k_1, k_2, k_3$  are four new derived coefficients which are combinations of the elements of rotation matrix  $R$  and the scaling factor  $\lambda$ .

The coefficients in (4) can be represented using two rotation angles  $\theta_1, \theta_2$ , a shift  $y_0$  and a mean-scaling factor  $s$ :

$$\begin{aligned} \theta_1 &= \arctan(k_0/k_1) \\ \theta_2 &= \arctan(k_2/k_3) \\ y_0 &= \pm 1/\sqrt{k_2^2+k_3^2} \\ s &= \sqrt{(k_0^2+k_1^2)/(k_2^2+k_3^2)} \end{aligned} \quad (5)$$

where a positive sign is chosen for  $y_0$  if  $k_3 > 0$  otherwise negative sign for  $y_0$  if  $k_3 \leq 0$ .

The above model was originally developed by the author for the purpose of fast epipolar image generation from uncertain projections, and has proven to be extremely useful when information about the imaging sensors is unavailable. Here, this model is logically adopted as the first model of proposed three-model approach.

From the ortho-rectification point of view, it can be shown that  $\theta_1 = -A$  and  $\theta_2 = k$ . A further assumption can be made that  $\theta_2 = 0$  (this is almost true for mirror and pushbroom line scanning sensors). The azimuth  $A$  and the shift  $y_0$  can then be estimated using the following simplified equations:

$$k_0 X + k_1 Y + k_3 y + 1 = 0 \quad (6)$$

The parameters are estimated by minimising the residual sum of squares for observations:

$$\sum (m_0 + m_1 X + m_2 Y - Y + y)^2 \rightarrow \min \quad (7)$$

where

$$k_0 = m_1/m_0, k_1 = (m_2 - 1)/m_0, k_2 = 0, k_3 = 1/m_0$$

### 3.2 Second Model

Assuming there is a overall pitch/shearing angle effect after applying the first model, the azimuth angle has been corrected (set to zero), and the properties of the coplanar are taken into account, then the following relationship can be derived from (1):

$$\sin \gamma \cdot x \cdot Y - \cos \gamma \cdot f \cdot Y + f \cdot y = 0$$

With further simplifications with  $k_4 = \sin \gamma / f$  and  $k_5 = -\cos \gamma$ , the above equation is equivalent to the following observation equation:

$$-y = x \cdot Y \cdot k_4 + Y \cdot k_5$$

The parameters  $k_4$  and  $k_5$  are estimated by minimising the residual sum of squares for observations:

$$\sum (x \cdot Y \cdot k_4 + Y \cdot k_5 + y)^2 \rightarrow \min \quad (8)$$

### 3.3 Third Model

The action of most satellite sensors can be regarded as a perspective-affine projection. After applying the first and second models, a third model, which is a perspective-affine transformation, is applied. The image roll angle  $\gamma$  and affine transformation coefficients  $s_x, s_y, s_0$  are treated as the four unknowns in (9):

$$X \cdot s_x + Y \cdot s_y + s_0 = Z_s \frac{\sec(\gamma)x - \cos(\gamma)x \frac{Z}{Z_s} - \sin(\gamma)Z}{\cos(\gamma)Z_s - \sin(\gamma)x} \quad (9)$$

or

$$\begin{cases} X \cdot s_x + Y \cdot s_y + s_0 = Z_s \frac{u}{v} \\ u = \sec(\gamma)x - \cos(\gamma)x \frac{Z}{Z_s} - \sin(\gamma)Z \\ v = \cos(\gamma)Z_s - \sin(\gamma)x \end{cases}$$

where  $Z_s$  is the satellite height.

The parameters are estimated by minimising the residual sum of squares for observations:

$$\sum (Z_s \frac{u}{v} - X \cdot s_x - Y \cdot s_y - s_0)^2 \rightarrow \min \quad (10)$$

Some common minimisation techniques can be applied for solving parameters  $\gamma, s_x, s_y, s_0$ . The least squares techniques are adopted here. After differentiating  $u$  and  $v$  with respect to  $\gamma$ , the observation equation with respected to the image roll angle  $\gamma$  and the affine transformation coefficients  $s_x, s_y, s_0$  is:

$$\begin{cases} v = Z_s \frac{du \cdot v - u \cdot dv}{v^2} d\gamma - X \cdot ds_x - Y \cdot ds_y - ds - b \\ du = \tan(\gamma) \sec(\gamma)x - \sin(\gamma)x \frac{Z}{Z_s} - \cos(\gamma)Z \\ dv = -\sin(\gamma)Z_s - \cos(\gamma)x \\ b = X \cdot s_x + Y \cdot s_y + s_0 - Z_s \frac{u}{v} \end{cases} \quad (11)$$

If taking into account the influence of the satellite roll angle  $\gamma$  related to scan-lines  $y$  (i.e.,  $\gamma_s = \gamma + y \cdot \Delta\gamma$ ), the observation equation could be written as follows:

$$v = Z_s \frac{du \cdot v - u \cdot dv}{v^2} d\gamma - X \cdot ds_x - Y \cdot ds_y - ds + y \cdot Z_s \frac{du \cdot v - u \cdot dv}{v^2} d\Delta\gamma - b \quad (12)$$

In summary, the steps of the three-model approach are:

- Find the azimuth  $A$  and shift  $y_0$  using (5) and (7);
- Estimate coefficients  $k_4, k_5$  using (8); and
- Estimate the image roll angle  $\gamma$ ,  $\Delta\gamma$  (if necessary) and affine coefficients  $s_x, s_y, s_0$  using (9) to (12).

Once model coefficients are estimated, the satellite image can then be ortho-rectified together using corresponding DEM data.

From the above model equations, it can be seen that there are only three unknowns in the first model, two unknowns in the second model, and four unknowns in the third. Because the three models are solved consecutively, a minimum of four ground control points are required. The small number of unknowns and minimal requirements for estimation make the three-model approach very easy to implement in practice.

In real applications, usually more than four well-distributed ground control points are available or can be acquired easily. We apply a robust estimation technique (Campbell et al, 1998) for estimating the unknowns from the available points. The robust estimation technique ensures estimated parameters are not affected by poor control points. This is advantageous for automation of the whole ortho-rectification process for large-scale production work.

**4. ORTHO-RECTIFICATION RESULTS AND COMPARISONS**

A commercially available software (PCI OrthoEngine) is chosen for the purpose of comparison. PCI OrthoEngine uses a rigorous satellite orbital model (Toutin’s Model) for satellite image ortho-rectification, and reads the satellite orbital auxiliary data associated with the satellite images. Results published by (Al-Rousan et al, 1997, Toutin, 1992, Toutin, et al, 2001, 2003) suggest that the PCI OrthoEngine is a versatile and highly accurate tool for almost every satellite sensor. Three trials were conducted in order to demonstrate their capabilities against the three-model approach.

**4.1 Test Imagery and Ground Control Points**

Three trials were conducted in order to compare the two ortho-rectification approaches. Trial A uses 12 Landsat TM 7 ETM+ scenes in the south-western region of Western Australia (Figure 1). Trial B uses 9 Landsat TM 7 ETM+ scenes in the Ord-Bonaparte region of Northern Territory, Australia (Figure 2). Trial C uses 2 SPOT4 scenes (a stereo pair) in the Pemberton area, in the south-western region of Western Australia (Figure 3).

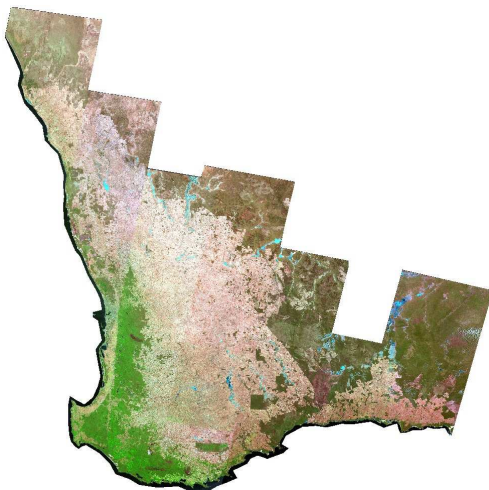


Figure 1. Trial A: Mosaicked ortho-rectified images of the south-western region, Western Australia (contains 12 Landsat TM 7 ETM+ scenes). RGB bands correspond to bands 5, 4 and 3, respectively.

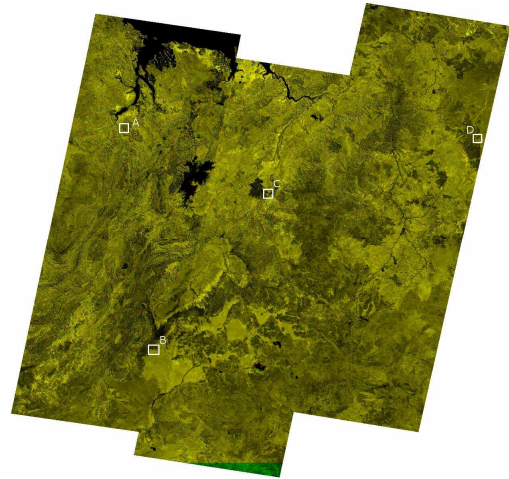


Figure 2. Trial B: Mosaicked ortho-rectified images of Ord-Bonaparte region of Northern Territory, Australia (contains 9 Landsat TM 7 ETM+ scenes). The red band is from PCI OrthoEngine and the green band is from the three-model approach.

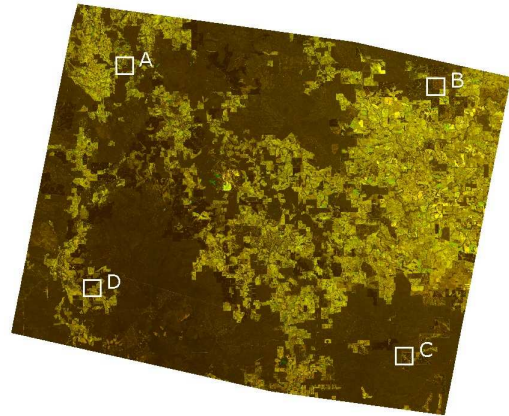


Figure 3. Trial C: 2 SPOT4 scenes (a stereo pair) in the Pemberton area, south-western region of Western Australia. The red band is from PCI OrthoEngine and the green band is from the proposed approach.

**4.2 Comparisons between PCI OrthoEngine and the Three-Model Approaches**

The numbers of ground control points (GCPs) used in the three trials and model fitting residuals are listed in Tables 1–3, respectively. It is worth mentioning that the GCPs were carefully examined by the operator using PCI’s graphical user interface, and those GCPs having large residuals (normally larger than 1.5 pixels, pixel size is 25 metres for Landsat TM 7 ETM+ and 10 metres for SPOT4) were eliminated manually. On contrast, GCPs having large residuals were automatically removed by the three-model approach after applying a robust estimation technique.

| Scene | PCI OrthoEngine |      |      | Three-Model Approach |      |      |
|-------|-----------------|------|------|----------------------|------|------|
|       | GCP             | RMSX | RMSY | GCP                  | RMSX | RMSY |
| 11479 | 207             | 12.9 | 10.1 | 188                  | 11.5 | 8.0  |
| 11380 | 194             | 13.5 | 8.1  | 221                  | 20.5 | 6.9  |
| 11381 | 250             | 16.9 | 9.7  | 242                  | 18.4 | 8.6  |
| 11281 | 248             | 17.4 | 7.9  | 246                  | 18.5 | 6.3  |
| 11283 | 235             | 14.5 | 9.1  | 228                  | 16.2 | 7.1  |
| 11181 | 235             | 11.5 | 8.4  | 241                  | 13.0 | 8.8  |

|             |     |      |      |     |      |      |
|-------------|-----|------|------|-----|------|------|
| 11183       | 158 | 7.9  | 6.6  | 156 | 9.4  | 5.8  |
| 11184       | 205 | 10.0 | 8.9  | 215 | 11.7 | 8.3  |
| 11082       | 205 | 12.8 | 14.1 | 226 | 20.1 | 16.4 |
| 10983       | 96  | 9.0  | 7.4  | 95  | 9.8  | 8.0  |
| 10883       | 166 | 12.0 | 9.2  | 155 | 13.0 | 9.3  |
| 10783       | 38  | 11.1 | 12.2 | 28  | 8.0  | 6.6  |
| Average RMS |     | 12.5 | 9.3  |     | 14.2 | 8.3  |

Table 1. Trial A: GCP root mean squares using PCI OrthoEngine and three-model approach (RMSX and RMSY are the root mean squares of easting and northing residuals, respectively. Unit are metres.)

| Scene       | PCI OrthoEngine |      |      | Three-Model Approach |      |      |
|-------------|-----------------|------|------|----------------------|------|------|
|             | GCP             | RMSX | RMSY | GCP                  | RMSX | RMSY |
| 10771       | 33              | 5.5  | 8.6  | 28                   | 4.0  | 4.6  |
| 10772       | 31              | 8.6  | 4.6  | 28                   | 5.2  | 3.8  |
| 10773       | 27              | 7.2  | 7.6  | 25                   | 4.9  | 5.1  |
| 10671       | 29              | 8.8  | 6.2  | 25                   | 4.7  | 5.2  |
| 10672       | 27              | 6.9  | 8.8  | 21                   | 8.9  | 5.5  |
| 10673       | 29              | 7.2  | 8.6  | 26                   | 6.4  | 7.1  |
| 10571       | 40              | 7.6  | 6.4  | 35                   | 7.6  | 6.4  |
| 10572       | 41              | 6.5  | 7.0  | 36                   | 5.3  | 4.1  |
| 10573       | 36              | 11.5 | 11.2 | 31                   | 9.3  | 10.0 |
| Average RMS |                 | 7.8  | 7.7  |                      | 6.2  | 5.7  |

Table 2. Trial B: GCP root mean squares using PCI OrthoEngine and three-model approach (RMSX and RMSY are the root mean squares of easting and northing residuals, respectively. Unit are metres.)

| Scene       | PCI OrthoEngine |      |      | Three-Model Approach |      |      |
|-------------|-----------------|------|------|----------------------|------|------|
|             | GCP             | RMSX | RMSY | GCP                  | RMSX | RMSY |
| Left        | 52              | 10.8 | 7.4  | 52                   | 11.5 | 7.5  |
| Right       | 52              | 11.5 | 9.1  | 52                   | 10.9 | 8.2  |
| Average RMS |                 | 11.1 | 8.2  |                      | 11.2 | 7.8  |

Table 3. Trial C: GCP root mean squares using PCI OrthoEngine and three-model approach (RMSX and RMSY are the root mean squares of easting and northing residuals, respectively. Unit are metres.)

Although the statistics listed in Tables 1–3 suggest that much closer results can be achieved by both approaches, the three-model approach eliminates more control points than PCI OrthoEngine does. It is fair to say that the average residuals of the three-model approach should be bigger than PCI OrthoEngine’s if the same mount of control points are used. It is explainable in that much more satellite ephemeris information was used in PCI OrthoEngine’s approach and that the three-model approach is not optimised for any particular satellite sensors whilst PCI OrthoEngine is.

As shown in the last rows of Tables 1–3, the average root mean squares of easting and northing residuals for the three trials (using PCI OrthoEngine) are:

- Trial A: 12.5m, 9.3m for easting and northing, respectively;
- Trial B: 7.8m, 7.7m for easting and northing, respectively;
- Trial C: 11.1m, 8.2m for easting and northing, respectively.

The average root mean squares of easting and northing residuals for the three trials (using the three-model approach) are:

- Trial A: 14.2m, 8.3m for easting and northing, respectively;
- Trial B: 6.2m, 5.7m for easting and northing, respectively;
- Trial C: 11.2m, 7.8m for easting and northing, respectively.

### 4.3 Visual Inspection on Ortho-Rectified Images

An easy way to compare the results in Trial A and B is to overlay two ortho-rectified images (setting the red band from PCI OrthoEngine and setting the green band from the three-model approach), and then visually check the alignment on some obvious features such as creeks, roads and edges. Images used in Trial B were carefully inspected using this visual check method. It is very promising that the visible misalignments are under one pixel (25 metres) in the majority of areas and two pixels (50 metres) only in very rare areas. Figure 4 shows overlaid sub-images of four randomly selected areas (illustrated in Figure 2).

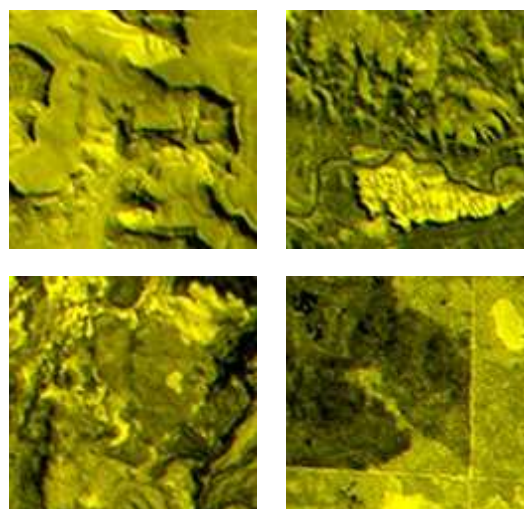
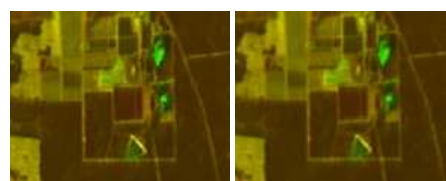
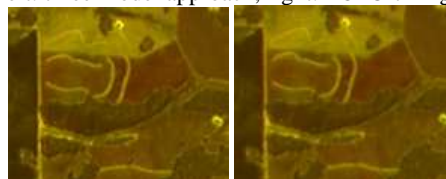


Figure 4. Trial B: The misalignments in sub-image areas (illustrated in Figure 2). Box A: top-left, Box B: top-right, Box C: bottom-left and Box D: bottom-right. (The red band is from PCI OrthoEngine and the green band is from the three-model approach.)

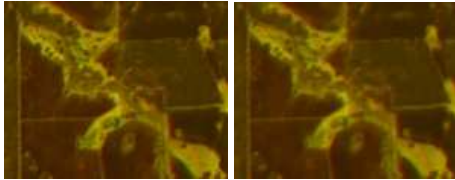
Another common way to compare the ortho-rectification results for stereo pairs is to overlay two ortho-rectified images (setting the red band from the left orthoimage and setting the green band from the right orthoimage), and then visually check the alignment in some features. Ortho-rectified images used in Trial C were carefully inspected using this method. Again, it is very promising that the visible misalignments are under one pixel (10 metres) in the majority of areas and two pixels (20 metres) only in very rare areas. Figure 5 shows overlaid sub-images of four randomly selected areas (illustrated in Figure 3).



Box A (left: three-model approach, right: PCI OrthoEngine)



Box B (left: three-model approach, right: PCI OrthoEngine)



Box C (left: three-model approach, right: PCI OrthEngine)



Box D (left: three-model approach, right: PCI OrthEngine)

Figure 5. Trial C: The misalignments between left and right ortho-rectified images from the three-model approach (the red band is the left image and the green band is the right image).

## 5. DISCUSSION

The results from the proposed three-model approach for satellite image ortho-rectification are very promising compared to the rigorous satellite orbital modelling approach.

The proposed three-model approach has a clear physical meaning for each model and the implementation is very simple. The biggest advantage of the three-model approach over other approaches is that it does not require: 1) any imaging sensor details such as the focal length or the pixel size; 2) the satellite orbit information such as the approximations of the satellite positions and view angles; and 3) additional coordinates transformation between the map-projection coordinate system and the local coordinate system. Only the approximation of satellite height is required for the proposed approach.

In addition to achieving good residuals, the proposed three-model approach is also bundled with a robust estimation technique. Two large trials demonstrated that the proposed approach is a good alternative choice for real production work.

Some improvements are being investigated. These include how to automatically retain good spatial distribution of control points whilst applying robust estimation technique to eliminate control points with large residuals. Since the current studies are mainly focused on Landsat TM and SPOT4 imagery, the application of the proposed approach to other types of satellite imagery, especially for the high-resolution satellite imagery such as IKONOS, QuickBird and ALOS imagery, needs to be included for further studies.

## 6. REFERENCES

Al-Rousan, N., Cheng P., Petrie, G., Toutin, T. and Valadan Zoej, M., 1997. Automated DEM Extraction and Orthoimage Generation from SPOT Level 1B Imagery. *Photogrammetric Engineering and Remote Sensing*, 63, No 8, pp.965-974.

Bannari, A., Morin, D., Benie, G. and Bonn, F., 1995. A Theoretical Review of Different Mathematical Models of Geometric Corrections Applied to Remote Sensing Images. *Remote Sensing Reviews*, 13, pp.27-47.

Campbell, N. A., Lopuhaa, H. P. and Rousseeuw, P. J., 1998. On the calculation of a robust S-Estimator of a Covariance Matrix. *Statistics in Medicine*, 17, pp.2685-2695.

Grodecki, J., 2001. Ikonos stereo feature extraction - RPC approach. *Proc. ASPRS Annual Conference*, St. Louis, 23-27 April 2001, 7 p. (on CD ROM).

Salamonowicz, P., 1986. Satellite Orientation and Position for Geometric Correction of Scanner Imagery. *Photogrammetric Engineering and Remote Sensing*, 52, No 4, pp.491-499.

Toutin, T., 1992. An Integrated Method to Rectify Airborne Radar Imagery Using DEM. *Photogrammetric Engineering and Remote Sensing*, 58, No 4, pp.417-422.

Toutin T., Carbonneau, Y. and Chenier, R., 2001. Block adjustment of Landsat-7 ETM+ images. *Proc. Joint ISPRS Workshop "High Resolution Mapping from Space 2001"*, Hannover, Germany, September 19-21.

Toutin, T., Chenier, R. and Carbonneau, Y., 2003. Multi Sensor Block Adjustment. *Proc. Geoscience and Remote Sensing Symposium (IGARSS)*, Vol.2, pp.1041-1043.

Wang, Z. Z., 1990. *Principles of Photogrammetry (with Remote Sensing)*. Publishing House of Surveying and Mapping, Beijing.